LETTER **Communicated by Simon Haykin**

Delay Differential Analysis of Electroencephalographic Data

Claudia Lainscsek
claudia@salk.edu
Howard Hughes Medical Institute, Computational Neurobiology Laboratory, Salk Institute for Biological Studies, La Jolla, CA 92037, U.S.A., and Institute for Neural Computation, University of California San Diego, La Jolla, CA 92093, U.S.A.

Manuel E. Hernandez
mhernand@illinois.edu
Institute for Neural Computation, University of California San Diego, La Jolla, CA 92903, U.S.A.

Howard Poizner
hpoizner@ucsd.edu
Institute for Neural Computation and Graduate Program in Neurosciences, University of California San Diego, La Jolla, CA 92903, U.S.A.

Terrence J. Sejnowski
terry@salk.edu
Howard Hughes Medical Institute, Computational Neurobiology Laboratory, La Jolla, CA 92037, U.S.A., and Institute for Neural Computation, University of California San Diego, La Jolla, CA 92903, U.S.A.

We propose a time-domain approach to detect frequencies, frequency couplings, and phases using nonlinear correlation functions. For frequency analysis, this approach is a multivariate extension of discrete Fourier transform, and for higher-order spectra, it is a linear and multivariate alternative to multidimensional fast Fourier transform of multidimensional correlations. This method can be applied to short and sparse time series and can be extended to cross-trial and cross-channel spectra (CTS) for electroencephalography data where multiple short data segments from multiple trials of the same experiment are available. There are two versions of CTS. The first one assumes some phase coherency across the trials, while the second one is independent of phase coherency. We demonstrate that the phase-dependent version is more consistent with event-related spectral perturbation analysis and traditional Morlet wavelet analysis. We show that CTS can be applied to short data windows and yields higher temporal resolution than traditional Morlet wavelet analysis. Furthermore, the CTS can be used to reconstruct the event-related potential using all linear components of the CTS.

Neural Computation **27, 615–627** (2015)
doi:10.1162/NECO_a_00656

1 Introduction

Tools that improve on the temporal or spatial resolution of existing human imaging technologies provide us with a better understanding of how neural activity shapes our behavior, as well as provides us with further insight into neurological diseases and disorders. Electroencephalography (EEG) provides a noninvasive time-series measure of cortical brain activity with excellent temporal resolution. However, existing frequency analysis and analysis of frequency and phase couplings in the time domain are poorly understood (Hjorth, 1970; Chan & Langford, 1982; Raghuveer & Nikias, 1985, 1986; Stankovic, 1994).

In a companion paper (Lainscsek & Sejnowski, 2015), we make the connection between nonlinear dynamics and spectral analysis using functional embeddings or delay differential equations (DDE) of time-series data. This idea was introduced by Lainscsek and Sejnowski (2013). We show how the properties of simple DDEs can be used for time-domain spectral and bispectral analysis. Considering a signal

$$x(t) = \mathcal{S} + \mathcal{P}\,; \quad \mathcal{P} = \cos(\Omega t + \phi). \tag{1.1}$$

where $\mathcal{S}$ is the signal under investigation and $\mathcal{P}$ is a probing signal, we demonstrate that the function $L(\Omega)$ for $\mathcal{S} = \sum_{i=1}^{\infty} A_i \cos(\omega_j t + \varphi_i)$, where

$$L(\Omega) = \max_{\phi} \left(\langle x^2 \rangle - \langle \mathcal{S}^2 \rangle - \frac{1}{2} \right), \tag{1.2}$$

can be used as a frequency detector, similar to the Goertzel algorithm (Goertzel, 1958; Jacobsen & Lyons, 2003). In the companion paper (Lainscsek & Sejnowski, 2015), we also give the theoretical basis for a novel time-domain bispectrum (TDB) $B(\Omega)$ for $\mathcal{S} = \sum_{i=1}^{\infty} A_i \cos(\omega_j t + \varphi_i) + A_{j,k} \cos((\omega_j + \omega_k) t + \varphi_j + \varphi_k)$ where

$$B(\Omega) = L(\Omega) \cdot \max_{\phi} \left(\langle x^3 \rangle - \langle \mathcal{S}^3 \rangle \right). \tag{1.3}$$

EEG data often contain trials with artifacts, or data segments that cannot be used for analysis. A benefit of equations 1.2 and 1.3 is that they can be used on data sparsely sampled in time. Thus, given a sparse signal $x(T)$, where T is the vector of times for which the signal is good, the probing signal $D\cos(\Omega T + \phi)$ can be used to detect the spectrum. Similarly, T can be used when very short segments of data need to be analyzed and there are multiple trials of the same experiment. Consider a signal $x_1(T_1), x_2(T_2), \ldots, x_n(T_n)$, where all time series $x_i(T_i)$ are centered around the same event, a stimulus S for EEG data (see the upper plot in Figure 1).

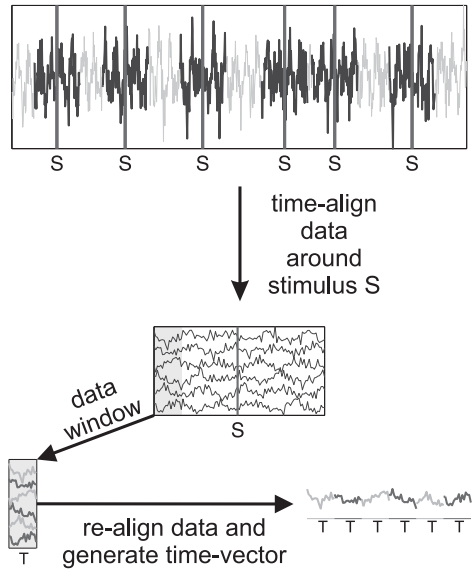

Figure 1: Realignment of data for the computation of a cross-trial spectrogram (CTS) that assumes some phase coherence in the data. First, the data are realigned around the stimulus S. Then for each data window, the data are concatenated and a new time vector is generated. The concatenated data are then the signal $\mathcal{S}$ in equation 1.1, and the new time vector is the time in the probing signal.

Then all time vectors T_i can be considered equal in duration and the signal can be concatenated as $x_1(T), x_2(T), \ldots, x_n(T)$ (see the middle plot in Figure 1). For a short data window that would be too short for frequency-domain spectral analysis, the data of all trials can be combined and the spectrum can be computed by using a probing signal with a time vector that consists of n repetitions of the time vector T for n data segments (see the lower plot in Figure 1). In this manner, a cross-trial spectrogram (CTS) can be computed using sliding short windows. This CTS version assumes phase coherency across the data segments. A cross-trial spectrogram can also be computed in a phase-independent manner by computing the spectrum of each time series in the data segment separately using equation 1.2 and then taking the mean over those spectra. As in the companion paper, we demonstrate the differences between the phase-dependent and the phase-independent versions of the CTS and the cross-trial bispectrum (CTB). However, in this letter, we use actual EEG data for comparing these novel applications to traditional wavelet and event-related spectral perturbation (ERSP) analyses.

The letter is organized as follows. Section 2 introduces the hardware used, the experimental setup, and the analysis; The results are described in section 3 and discussed in section 4.

2 Materials and Methods

2.1 Hardware. Electroencephalographic (EEG) data were collected using a 70-channel active electrode EEG system (Biosemi Inc. ActiveTwo, Amsterdam, Netherlands) consisting of a cap plus four EOG electrodes, temporal to both eyes and above and below the right eye; two EMG electrodes on the trapezius and right and left sternocleidomastoids; and two reference electrodes on the left and right mastoids. Data were recorded with a 512 Hz sampling rate and referenced to the averaged mastoid electrodes. Head position relative to the EEG sensors was determined with a electromagnetic motion tracking system (Polhemus, FASTRAK, Colchester, VT).

2.2 Participants. Nine healthy older adults (four females) participated in this study (mean $\pm$ SD age: 64.3 $\pm$ 7.9 years). No participant had any neurological or psychiatric disease. All participants were right-hand dominant with normal or corrected-to-normal vision. All participants signed the informed-consent document approved by the human subjects Institutional Review Board of the University of California, San Diego.

2.3 Protocol. Participants reached for and grasped a virtual rectangular object (3.5 $\times$ 8.5 $\times$ 6 cm) with haptic feedback provided to the thumb and index finger by two 3-degree-of-freedom haptic robotic devices (Phantom Premium 1.0, Geomagic, Wilmington, MA). Participants placed the digits of their right hand on a virtual starting dock and at the sound of a tone reached for the object at a comfortable speed. The object was located 13 to 18 cm away in a virtual environment designed using custom scripts (Vizard, WorldViz LLC, Santa Barbara, CA; Snider, Plank, Lee, & Poizner, 2011). Participants were provided haptic as well as visual feedback of the dock so that they felt their hands resting on a solid surface. Overall, a maximum of 360 (10 blocks of 36 trials) trials were performed by each participant, with rest provided between blocks to limit fatigue. In this study, we considered EEG data from 50 randomly selected trials from 1 second before the tone stimulus (S) to 1 second after the stimulus (see Lukos et al., 2013, for a detailed description of experimental procedures and behavioral results).

2.4 Data Processing and Analysis. In this study, we analyzed both raw and clean backprojected EEG data. To get clean data, raw EEG data were first imported into EEGLAB using Matlab (MathWorks, Natick, MA) for processing (Delorme & Makeig, 2004). Data were then high-pass-filtered at 1 Hz to remove drift and low-pass-filtered at 55 Hz to remove line noise.

EEG artifacts associated with eye and other muscle movement were removed using independent component analysis (ICA) (Jung et al., 2000). Based on the topography, spectra, and trial-to-trial characteristics of ICA components, nonartifactual components were selected and used to generate backprojected EEG data.

The rearranged EEG data (see Figure 1) from the Cz electrode were used for the cross-trial time-domain frequency analysis. We first evaluated the effect of the data window size on the performance of the phase-dependent CTS using 1 to 40 trials of varying sizes (i.e., 16 to 1000 ms). The phase-dependent CTS can be used to detect frequencies with windows as small as 31 ms from a single trial and 16 ms with 40 trials of time series data sampled at 512 Hz. We then computed CTS with data windows of only 100 ms in length with a window shift of 10 ms. This consisted of only 50 data points (the sampling rate was 512 Hz) for each trial. However, when we used 50 trials and realigned each data window as shown in Figure 1, there were then $50 \times 50 = 2500$ data points in each data window. We compared this CTS to both traditional Morlet wavelet analysis (Mallat, 2008) and ERSP analysis (Makeig, 1993). The computation time of all of these methods is very similar. The ERSP measures average dynamic changes in amplitude of the broadband EEG frequency spectrum as a function of time relative to an event of interest.

To compute an ERSP, we calculated baseline spectra from the EEG immediately preceding each event. The epoch was divided into overlapping data windows, and a moving average of the amplitude spectra of these was created. Each of these spectral transforms of individual response epochs was then normalized by dividing by their respective mean baseline spectra. Normalized response transforms for many trials were then averaged to produce an average ERSP. We calculated ERSP using a fast Fourier transform on EEGLAB with default parameters.

We also discuss a method for interpreting nonlinear couplings in EEG data and demonstrate a potential application of the phase-dependent CTS in the reconstruction of salient event-related potential characteristics.

3 Results

As a proof of concept, Figure 2 shows the traditional Morlet wavelet spectrogram, phase-dependent CTS, phase-independent CTS, and CTB from nine participants. All three methods identify theta (4–8 Hz) and alpha (8–12 Hz) activity after the tone stimulus. However, in contrast to Morlet wavelets, CTS is able to provide finer temporal resolution and suggests increased phase coherence at 200 ms after the tone stimulus, based on the phase-independent CTS. The correlation coefficient between Figures 2b and 2c is 0.6 on average, with correlations ranging from 0.1 in C004 to 0.9 in C006, suggesting large variations in the overall phase coherence across participants. Furthermore, Figure 3 shows all four methods on the raw, unprocessed EEG

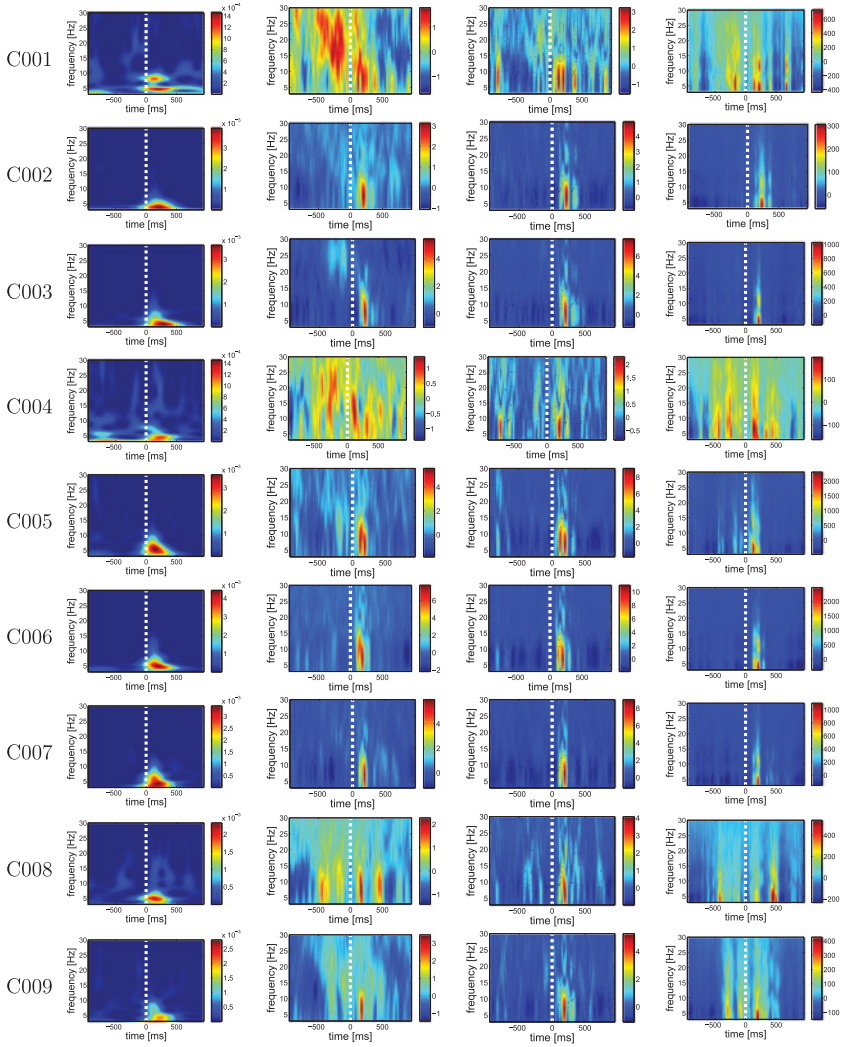

Figure 2: Frequency spectra time-locked to a stimuli onset (dashed white line) in the Cz electrode for the (a) Morlet wavelet spectrogram, (b) phase-dependent cross-trial spectrogram (CTS), (c) phase-independent CTS, and (d) cross-trial bispectrum (CTB), based on 50 randomly selected trials.

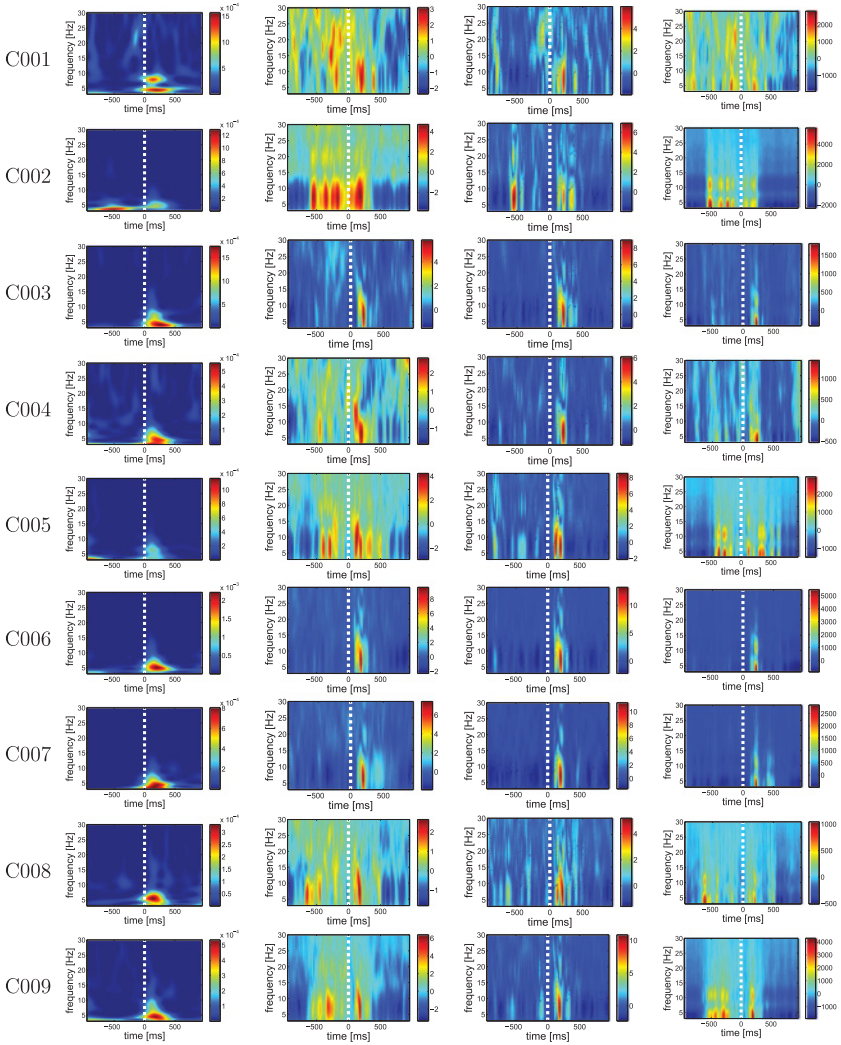

(a) Morlet wavelet spectrogram (b) phase-dependent CTS (c) phase-independent CTS (d) CTB

Figure 3: Frequency spectra of raw, unprocessed EEG data from the previously selected trials in Figure 2 time-locked to a stimuli onset (dashed white line) in the Cz electrode, for the (a) Morlet wavelet spectrogram, (b) phase-dependent cross-trial spectrogram (CTS), (c) phase-independent CTS, and (d) cross-trial bispectrum (CTB).

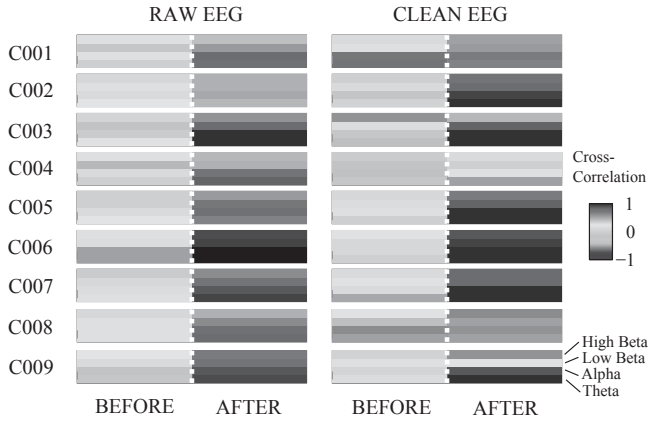

Figure 4: Coherence analysis before and after the stimulus (S) in raw and clean EEG data in theta (3–8 Hz), alpha (8–12 Hz), and low (12–20 Hz) and high (20–30 Hz) beta frequency bands using the cross-correlation between the phase-dependent and phase-independent CTS.

data. The mean correlation coefficient between Figures 3b and 3c is also 0.6, suggesting phase coherence, consistent with clean EEG data. The similarity between clean and raw EEG data is evident in the CTB, as frequency couplings are indicated in the delta, low theta, and alpha frequency ranges approximately 200 ms after the stimuli.

Furthermore, the use of specific time and frequency windows of interest allows coherence analysis using the phase-dependent and phase-independent CTS. Using four clinically relevant frequency bands, theta (3–8 Hz), alpha (8–12 Hz), and low (12–20 Hz) and high (20–30 Hz) beta, we can examine changes in phase coherence before and after the stimulus. As seen in Figure 4, there is significant coherence in theta, alpha, and beta bands after the tone (i.e., mean correlation ranges from 0.59 to 0.82), which is in contrast to data before the tone (mean correlation ranges from 0.17 to 0.26). Applying the same methodology to raw data demonstrated similar results, with cross-correlations between the phase-dependent and phase-independent CTS ranging from 0.56 to 0.80, further demonstrating the robustness of this measure to noise in certain experimental circumstances and populations.

We found phase-dependent CTS to be consistent with ERSP analysis for both clean and raw data (see Figure 5), as the stimuli elicited an increase in low-frequency neural activity, in delta (0.5–4 Hz), theta (4–8 Hz), and alpha (8–12 Hz) bands (see Figure 2). Comparing clean to raw EEG data demonstrates similarities in the dominant frequencies detected in the signal, particularly in the lower frequencies. As expected, the time course of the

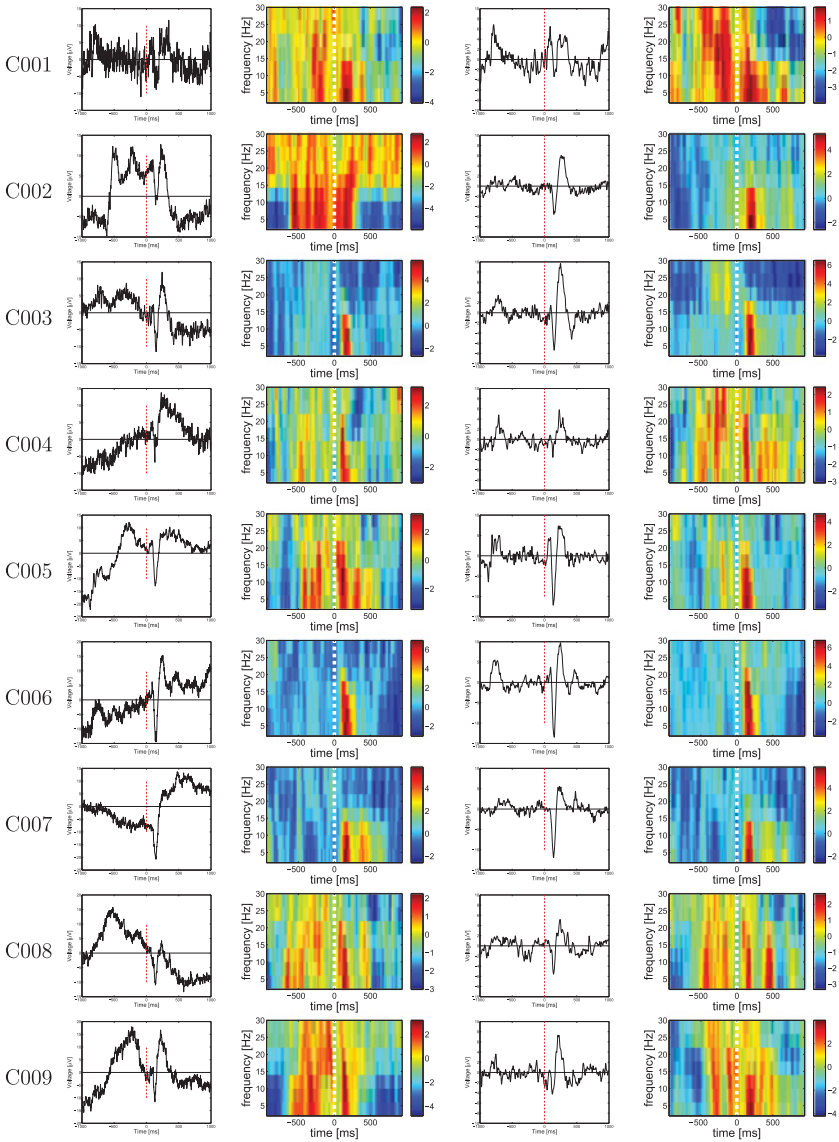

Figure 5: Event-related potentials (ERP) and event-related spectral perturbations (ERSPs) on (a, b) raw and (c, d) clean data, demonstrating low-frequency activity after the stimuli (S) in both raw and clean EEG data.

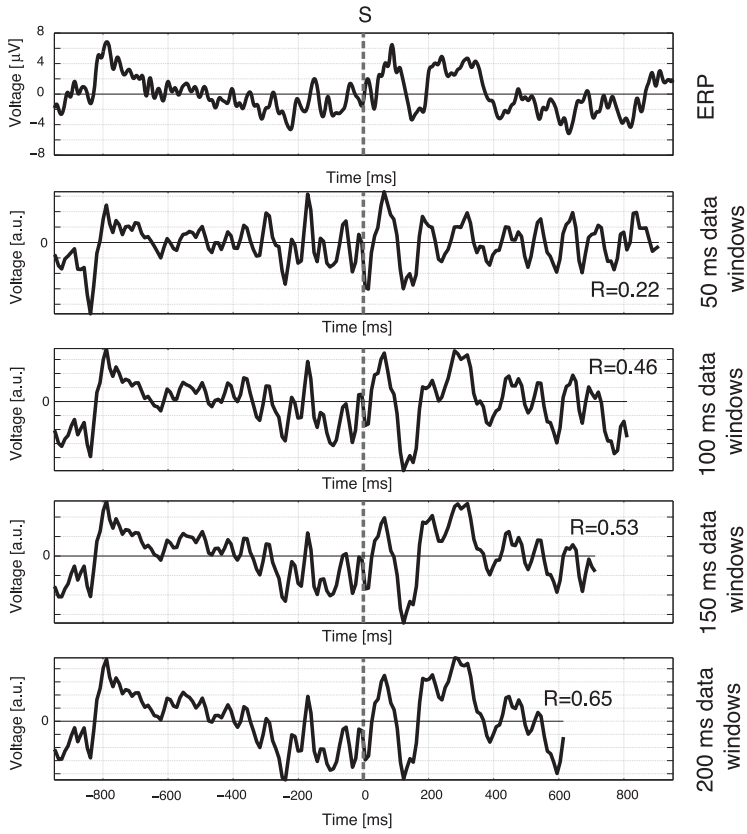

Figure 6: Event-related potential (ERP) time-locked to stimuli (top) and representative ERP reconstructions using 50, 100, 150, and 200 ms data windows. As the data windows increase, more of the lower-frequency characteristics of the ERP such as the negative drift prior to the tone onset are recovered, as measured by the increased cross-correlation between the original and the reconstructed ERP.

event-related potential (ERP) is dominated by high-frequency noise and drift in the raw data, but reveals what may be interpreted as an auditory N1 (negative 100 ms latency ERP) and a positive event-related potential with a 200 ms latency after the stimuli in clean EEG data (Luck, 2005).

In addition, using only the phase-independent CTS, we can reconstruct salient features of the event-related potential (see Figure 6). Increasing the size of the data window from 50 to 200 ms leads to nearly a three-fold increase in cross-correlation between the original and reconstructed ERP (i.e., R = 0.22 to 0.65). Thus, using only a subset of linear features from the

phase-independent CTS can still provide a significant amount of information about the underlying EEG signal.

4 Discussion

CTS analysis can distinguish changes in frequency in a broadband physiological signal using only sparse, short time segments. In contrast to traditional wavelet and ERSP analysis, the current CTS analysis is capable of using shorter data windows and thus allows finer temporal resolution in the frequency analysis of EEG signals. However, further work remains to assess the sensitivity of this method on broadband systems and similarities and contrasts to other existing frequency analysis methods. This time-domain frequency analysis tool appears to be promising for use in future applications of noisy and complex signals, such as EEG, where a measure of rapid changes in frequency is desired.

Furthermore, CTS analysis provides a measure of phase coherence that can be applied to quantify EEG phase coherence changes due to experimentally controlled stimuli in clinically relevant frequencies that may be applicable to differentiating between patients with and without neurological disorders (Farmer, 2002; Tcheslavski & Beex, 2006; Doesburg, 2009). In contrast to traditional wavelet analysis, CTS can be applied to sparse data, similar to discrete Fourier transform (DFT), as long as the data satisfy the restrictions of the Nyquist theorem (Nyquist, 1928). In contrast to traditional ERSP analysis, CTS uses the data of each data window of many trials simultaneously to compute the spectrogram, while ERSP averages over individual spectra. Therefore, CTS can use shorter data windows if enough trials are available, while ERSP is restricted to the minimum window length for each spectrum. Similar to Thompson's multiple-window time-frequency analysis (Xu, Haykin, & Racine, 1999), phase-independent CTS allows time-frequency phase coupling to be obtained from a single realization, but with improved temporal and frequency resolutions.

The CTB computes a time-domain bispectrum across channels or trials in a linear way and provides a novel tool for interpreting bicorrelations and higher-order statistics in EEG (Lainscsek & Sejnowski, 2015). The use of new methods that incorporate not only second-order but also higher-order statistics allows applications to noisy nonlinear systems (Principe, 2010).

5 Conclusion

We have introduced a new set of time-domain tools to analyze the frequency content and frequency coupling in stochastic signals: the time-domain spectrum (TDS), the time-domain bispectrum (TDB), the time-domain cross-trial (or cross-channel) spectrogram (CTS), and the time-domain cross-trial (or cross-channel) bispectrogram (CTB). In addition, the CTS has a phase-dependent and a phase-independent realization. Together, this

time-domain toolbox provides higher temporal resolution and increased phase coupling information, and it allows an easy and straightforward implementation of higher-order spectra across time compared with frequency-based methods such as Morlet wavelet analysis and cross-spectral analysis.

Acknowledgments

We acknowledge support by the Howard Hughes Medical Institute, NSF grant SMA-1041755, NSF ENG-1137279 (EFRI M3C), NIH grant 2 R01 NS036449, NS040522, the Swartz Foundation and ONR MURI award: N00014-10-1-0072. We also thank Jonathan Weyhenmeyer for valuable discussion on this letter and Xin Wang for helping with the wavelet analysis.

References

Chan, Y., & Langford, R. (1982). Spectral estimation via the high-order Yule-Walker equations. *IEEE Transactions on Acoustics, Speech and Signal Processing*, *30*(5), 689–698.

Delorme, A., & Makeig, S. (2004). EEGLAB: An open source toolbox for analysis of single-trial EEG dynamics including independent component analysis. *J. Neurosci. Methods*, *134*(1), 9–21.

Doesburg, S. (2009). Synchronization between sources: Emerging methods for understanding large-scale functional networks in the human brain. In J. Velazquez & R. Wennberg (Eds.), *Coordinated activity in the brain: Measurements and relevance to brain function and behavior* (vol. 2, pp. 25–42). New York: Springer.

Farmer, S. (2002). Neural rhythms in Parkinson's disease. *Brain*, *125*(6), 1175–1176.

Goertzel, G. (1958). An algorithm for the evaluation of finite trigonometric series. *American Mathematical Monthly*, *65*(1), 34–35.

Hjorth, B. (1970). EEG analysis based on time domain properties. *Electroencephalography and Clinical Neurophysiology*, *29*(3), 306–310.

Jacobsen, E., & Lyons, R. (2003). The sliding DFT. *IEEE Signal Processing Magazine*, *20*(2), 74–80.

Jung, T., Makeig, S., Humphries, C., Lee, T., McKeown, M., Iragui, V., & Sejnowski, T. (2000). Removing electroencephalographic artifacts by blind source separation. *Psychophysiology*, *37*(2), 163–178.

Lainscsek, C., & Sejnowski, T. (2013). Electrocardiogram classification using delay differential equations. *Chaos*, *23*(2), 023132.

Lainscsek, C., & Sejnowski, T. J. (2015). Delay differential analysis of time series. *Neural Computation*, *27*(3), 594–614.

Luck, S. (2005). *An introduction to the event-related potential technique*. Cambridge MA: MIT Press.

Lukos, J., Snider, J., Hernandez, M., Tunik, E., Hillyard, S., & Poizner, H. (2013). Parkinson's disease patients show impaired corrective grasp control and eye-hand coupling when reaching to grasp virtual objects. *Neuroscience*, *254*, 205–221.

Makeig, S. (1993). Auditory event-related dynamics of the EEG spectrum and effects of exposure to tones. *Electroencephalography and Clinical Neurophysiology*, *86*, 283–293.

Mallat, S. (2008). *A wavelet tour of signal processing: The sparse way* (3rd ed.). Orlando, FL: Academic Press.

Nyquist, H. (1928). Certain topics in telegraph transmission theory. *Trans. AIEE*, *47*, 617–644.

Principe, J. (2010). *Information theoretic learning: Renyi's entropy and kernel perspectives*. New York: Springer.

Raghuveer, M., & Nikias, C. (1985). Bispectrum estimation: A parametric approach. *IEEE Transactions on Acoustics, Speech and Signal Processing*, *33*(5), 1213–1230.

Raghuveer, M. R., & Nikias, C. L. (1986). Bispectrum estimation via AR modeling. *Signal Processing*, *10*(1), 35–48.

Snider, J., Plank, M., Lee, D., & Poizner, H. (2011). Simultaneous neural and movement recording in large-scale immersive virtual environments. In *Proceedings of Biomedical Circuits and Systems Conference* (pp. 98–101). Piscataway, NJ: IEEE.

Stankovic, L. (1994). A method for time-frequency analysis. *IEEE Transactions on Signal Processing*, *42*(1), 225–229.

Tcheslavski, G. V., & Beex, A. L. (2006). Phase synchrony and coherence analyses of EEG as tools to discriminate between children with and without attention deficit disorder. *Biomedical Signal Processing and Control*, *1*(2), 151–161.

Xu, Y., Haykin, S., & Racine, R. (1999). Multiple window time-frequency distribution and coherence of EEG using Slepian sequences and hermite functions. *IEEE Transactions on Biomedical Engineering*, *46*(7), 861–866.

Received November 21, 2013; accepted May 19, 2014.